

PCCP

Accepted Manuscript



This is an *Accepted Manuscript*, which has been through the Royal Society of Chemistry peer review process and has been accepted for publication.

Accepted Manuscripts are published online shortly after acceptance, before technical editing, formatting and proof reading. Using this free service, authors can make their results available to the community, in citable form, before we publish the edited article. We will replace this *Accepted Manuscript* with the edited and formatted *Advance Article* as soon as it is available.

You can find more information about *Accepted Manuscripts* in the [Information for Authors](#).

Please note that technical editing may introduce minor changes to the text and/or graphics, which may alter content. The journal's standard [Terms & Conditions](#) and the [Ethical guidelines](#) still apply. In no event shall the Royal Society of Chemistry be held responsible for any errors or omissions in this *Accepted Manuscript* or any consequences arising from the use of any information it contains.

DFT study of carbon monoxide adsorption on hydroxylated α - $\text{Al}_2\text{O}_3(0001)$ surfaces.

C. Rohmann¹, J.B. Metson¹ and H. Idriss^{2,3*}

¹School of Chemical Sciences, The University of Auckland, Auckland, New Zealand.

²Department of Chemistry, The University of Aberdeen, Aberdeen, UK

³SABIC CRI at KAUST, Thawal, Saudi Arabia.

*Email: h.idriss@abdn.ac.uk and idriss@sabic.com

Abstract

The adsorption of CO on the hydroxylated α - $\text{Al}_2\text{O}_3(0001)$ surface was studied using density functional theory (DFT). Dissociated adsorption of water was found to be stable; with an adsorption energy (E_a) of 1.62 eV at $\theta_{\text{water}} = 0.75$. The most stable hydroxylation form on the clean surface was found to be in the 1-2 dissociation configuration, where the OH group binds to a surface Al ion and the H ion binds to one of the three equivalent surface O ions. The adsorption energy of CO was found to be dependent on the degree of pre-hydroxylation of the surface as well as on the CO coverage. The highest adsorption energy of CO was found when $\theta_{\text{CO}} = 0.25$ onto a pre-hydroxylated surface with $\theta_{\text{water}} = 0.25$; $E_a = 0.57$ eV. The adsorption energy of CO decreased with increasing the degree of pre-hydroxylation. Vibrational frequency of ν_{CO} was also computed and in all cases it was blue shifted with respect to gas-phase CO. The shift, $\Delta\nu$, decreased with increasing CO coverage but increased with increasing surface hydroxylation. Comparison with available experimental work is discussed.

1. Introduction

The high temperature ceramic α - Al_2O_3 possesses good mechanical properties, is highly inert, and is used in a wide varieties of technological application¹. Furthermore, it is applied as a substrate for thin films as well as a support for transition metals in many important classes of catalysts^{2, 3}. Therefore, obtaining quantitative and qualitative information of the nature of interaction with adsorbates and the effects of surface reconstructions would enhance our understanding of catalytic reactions and materials properties.

The electronic structure of α - $\text{Al}_2\text{O}_3(0001)$ has seen experimental interest for many years^{4, 5}. Ahn and Rabalais⁴ studying the (0001) surface, by means of time-of-flight scattering and recoiling spectrometry, atomic force microscopy (AFM) and ion trajectory simulations, reported the (1 x 1) surface to be Al-terminated. Several computational studies^{6, 7} also showed that the Al-terminated surface is energetically the most stable. The wide use of α - Al_2O_3 as a common support in heterogeneous catalysis has led to many studies of the adsorption of transition metals, for example, Cu^{8, 9}, Pd^{8, 10} and Pt¹¹. Łodziana and Nørskov

2

investigated the adsorption of one monolayer of Pd and Cu metals over stoichiometric α - $\text{Al}_2\text{O}_3(0001)$ surface by means of density functional theory (DFT) with the GGA-PW91 exchange-correlation functional, reporting similar energies ($0.9\text{-}1.0\text{ J/m}^2$) for metal atoms preferring to occupy the hcp sites over the surface oxygen atoms. The adsorption of metals results in relatively large surface relaxations, where the topmost surface aluminium ions move towards the metals. In presence of surface hydroxyls, Pd and Cu exhibit a weak binding to the surface⁸. However, XPS studies investigating the adsorption of Cu onto the hydroxylated (0001) surface, report an enhanced binding of Cu to the surface due to the presence of surface hydroxyls^{12, 13}.

There have been several studies involving the adsorption of small molecules onto the α - $\text{Al}_2\text{O}_3(0001)$ surface. Investigations conducted on HCl^{14, 15} reported dissociative adsorption to be favoured. As in the case of transition metals, considerable surface relaxation is seen. Another molecule of interest is phenol¹⁶ which was computed for, using the semi-local density functional theory. The adsorption of phenol results in a binding separation (distance between surface Al and the O of the phenol molecule) of 1.95 \AA and an adsorption energy of 1.00 eV , with the energy increasing to around 1.2 eV when the contribution from van der Waals interactions is accounted for. Sorescu *et al.* investigating the adsorption of nitromethane on the (0001) surface of α - Al_2O_3 ¹⁷ reported the most stable configuration to occur when the molecule lays parallel to the surface and bonding with one O atom of the nitro group to the surface Al atom. Moreover adsorption in a parallel configuration was found to be 0.3 eV more stable compared to its vertical counter parts. The authors suggest that the increase in binding energy may be attributed to the repositioning of two H atoms of the methyl group which are pointing directly to the surface O atoms¹⁷.

Another molecule of great importance is water, which is present in molecular or dissociated form in the overwhelming amount of work conducted on metal oxide surfaces. In the case of corundum H ions were found to be present at temperatures as high as 1100°C ⁴. Moreover it was found that the clean, H free, Al terminated (0001) surface of Al_2O_3 readily reacts with water to form surface hydroxyls¹⁸⁻²³. Water is found to be strongly and dissociatively adsorbed; with energies close to 30 kcal/mol (ca. 1.3 eV) depending on the local binding sites²². A 1-2 dissociated state in which H^+ of H_2O binds to O_s , the nearest neighbour surface O of Al to which the OH^- of the same H_2O binds is found the most stable. This was followed

by a 1-4 dissociated state in which the surface O_s is across a 6-fold ring from this Al. Adsorption is accompanied by a strong relaxation of the surface. Thomas and Richardson showed that over a hydroxylated thin film surface, water does not totally wet the surface as less than 50 % of the surface is covered even at exposure equivalent to 7 monolayer²⁴.

A DFT study has considered a set of water adsorption and dissociation intermediates along the path from the dry to the fully hydroxylated surface²³. A molecular water layer was found to saturate at $2H_2O/Al_s$, with half the water bound through O to Al_s and the other half bound through H to O_s , forming a hexagonal, hydrogen-bonded water “bilayer” above the alumina plane. These molecular water states were found to be metastable. Water is reported to dissociate with its OH fragment atop Al_s and H fragment atop O_s . The dissociation of molecularly adsorbed water to the favoured 1-2 chemisorbed state was computed by means of the climbing image nudge elastic band (CI-NEB) method to determine the minimum energy path and transition state, and found to have a modest activation barrier of 0.19 eV²³.

CO is among the most commonly investigated probe molecule revealing fundamental information, such as surface structure, adsorbate-surface interaction, adsorption behaviour and coverage dependent CO vibrational shifts on a variety of metals, semi conductors and insulators. Computationally, it has been studied on many oxide systems, including α - $Al_2O_3(0001)$ ^{25, 26}, $Cu_2O(111)$ ²⁷, MgO ²⁸, CeO_2 ²⁹, and TiO_2 ^{30, 31}. In addition, it has been experimentally studied on a considerable number of metal oxides mainly by vibrational spectroscopic methods³²⁻³⁶. CO adsorption on transition metals such as Pt³⁷ causes a weakening of the CO bond, which in turn results in shifting the frequency of the CO bond to lower wavenumbers (red shifted) with respect to that of gas-phase CO. Its adsorption on metal oxides without d electrons in the valence band such as TiO_2 ³² strengthens the CO bond. Upon an increasing coverage significant changes in the vibrational frequency of adsorbed CO have been reported, for example, the adsorption on ZnO ³⁸, α - and γ - Al_2O_3 ^{26, 39, 40}, TiO_2 ³⁴, and $Pt(111)$ ³⁷.

The adsorption of CO onto Al_2O_3 was computationally studied using an Al_8O_{12} cluster model²⁵. The configuration with the bond through the C moiety of CO and the Al surface is the most stable. The bond is mainly due to σ donation to the $3p_z$ and $3d_z^2$ orbitals from the CO adsorbate to the Al surface. The adsorption energy was found close to 0.6 eV, while the vibrational frequency of adsorbed CO (ν CO mode) was blue shifted with respect to the gas-phase molecule (44 cm^{-1}). In our previous study²⁶, studying the coverage dependent

adsorption of CO onto the (0001) surface of α -Al₂O₃, a blue shift, with respect to gas phase CO, of 56 cm⁻¹ and 30 cm⁻¹ was observed for the lowest and highest coverage investigated, respectively. Experimental infrared (IR) works for CO interaction with powder α -Al₂O₃^{33, 41} indicated a blue shift of 20 to 40 cm⁻¹ with respect to gas phase CO.

In this work we present a study of the adsorption of CO onto hydroxylated (0001) surface of α -Al₂O₃. In particular, we focus on surface relaxation, the electronic structure upon CO adsorption and the change of the vibrational frequency of CO with respect to different surface coverage of CO and water.

2. Computational Details

Calculations were conducted using the plane-wave DFT calculations as implemented in the CASTEP (Cambridge Serial Total Energy Package) simulation package⁴². Electron exchange and correlation are described using the Perdew-Burke-Ernzerhof (PBE)⁴³ functional of the generalized gradient approximation (GGA). For the k-point sampling of the Brillouin zone, Monkhorst-Pack grids⁴⁴ were used. Ultrasoft pseudopotentials⁴⁵ were employed to lower the required basis set size. A cut-off of 400 eV was used for the bulk, (1 × 1), and (2 × 2) surfaces of α -Al₂O₃. A (5 × 5 × 2) set of k-points for the bulk and a (3 × 3 × 1) set for the surface calculations were used, while (6 × 6 × 1) for the (1 × 1) surface. To account for the insulating behaviour of Al₂O₃, the electronic occupation numbers were fixed during minimization. Atomic positions were optimized using the BFGS algorithm⁴⁶ with an energy convergence criterion of 5.0 × 10⁻⁶ eV/atom, a force convergence criterion of 0.01 eV/Å and a displacement convergence criterion of 5 × 10⁻⁴ Å were applied.

The crystal structure of α -Al₂O₃ can be described as a rhombohedral unit cell containing two formula units of Al₂O₃ with lattice parameters $a = 5.128$ Å and $\alpha = 55.29^\circ$. This corundum structure can also be described as a hexagonal cell, containing six formula units of Al₂O₃ having the lattice parameter $a = 4.760$ Å and $c = 12.989$ Å.

To validate our computational parameters, the optimized bulk lattice parameters, bulk modulus, and the cohesive energy of α -Al₂O₃ have been computed for. All values obtained were in good agreement with the previous experimental and computational works conducted on α -Al₂O₃^{14, 26, 47, 48}. A detailed listing and comparison of these values can be found in our previous investigation regarding the coverage dependent CO adsorption onto the clean α -Al₂O₃(0001) surface²⁶.

In order to compute for the vibrational frequency of CO adsorbing onto the hydroxylated Al₂O₃(0001) surface, the Dunham analysis was employed⁴⁹. While simulating the CO/OH

vibration, by changing the C-O/O-H bond distance in steps of 0.02 Å, the centre of weight was kept throughout the entire process. The presented results were obtained using a quartic fit of 7 points.

3. Results and Discussion

3.1 Free H₂O and CO

Calculations of gas-phase CO and H₂O at the gamma point were performed by placing the molecule in a cubic cell of 10 Å. In the case of water an O-H bond length of 0.977 Å and an H-O-H angle of 104.48° were obtained. Both values are in good agreement with those found by experimental⁵⁰ and computational⁵¹ investigations. The free CO molecule revealed a bond length of 1.154 Å also in agreement with previous studies²⁵ and a C-O stretching vibration of 2170 cm⁻¹ which is shifted by 27 cm⁻¹ with respect to the experimental value of 2143cm⁻¹. In a 10 × 10 × 10 Å³ cell the energy of free H₂O molecule is equal to -468.77 eV while that of free CO molecule is -590.16 eV.

3.2. α-Al₂O₃(0001) surface

Following our previous work²⁶, the (0001) surface is described by an 18 layer thick slab (six stoichiometric layers) where the top 11-layer were allowed to relax while the seven bottom layers were frozen at the bulk geometry; a 14 Å vacuum layer was added.

Consistent with other studies^{8, 47, 52, 53}, the optimised clean surface reveals a strong inward relaxation of the top Al layer into the following O layer, resulting in a decrease in the Al-O bond length. This strong inward relaxation, caused by charge redistribution from Al to O⁷, is responsible for the large difference in surface energy between the relaxed and unrelaxed structures; 1.54 J/m² and 3.50 J/m², respectively.

By comparing the density of states (DOS) of the bulk and the relaxed surface, a splitting of the bands in the 7 to 12 eV region is seen in addition to a decrease of the band gap by ca. 2 eV²⁶.

3.3. CO adsorption onto the (0001) surface

The adsorption of CO onto the (0001) surface of α-Al₂O₃ was previously studied; the main observations are summarised in the following:

The most stable CO adsorption is found at the lowest coverage investigated; 25 %. The vibrational frequency of ν CO revealed a coverage dependent blue shift with respect to gas phase CO in line with powder experimental work conducted on ZnO³⁸ and TiO₂³⁴. All

examined adsorbate coverage revealed a partial relieve of the strong relaxation on the Al adsorption site interacting with a CO molecule; this relieve was found to increase with decreasing CO coverage. The change in the adsorption energy of CO on the surface is best explained as due to changes in surface structure and not due to lateral CO interactions. A summary of the structural and vibrational changes upon different CO coverage is provided in Table SM1.

3.4. The hydroxylated (0001) surface of α -Al₂O₃

As mentioned in the introduction section, the Al terminated (0001) surface of Al₂O₃ readily reacts with water to form surface hydroxyls¹⁸⁻²³.

The dissociated H₂O molecule was placed in the 1-2 configuration, the OH group on top of the Al adsorption site and the H on top of one of the nearest neighbour O (Figure 1). (2 × 2) and (1 × 2) surfaces were employed to study water coverage of 25 %, 50 %, 75 % and 100 %. In good agreement with previous works with respect to surface geometry and adsorption energy^{22, 23}, we found that water adsorption onto the (1 × 1) surface (100 % coverage) is stable in the 1-2 configuration, exhibiting an adsorption energy of 1.45 eV. Table 1 presents the changes in interlayer distance upon adsorption of the OH⁻ group to the surface Al atom. The OH group binding to the top of the surface Al layer relieves the strong surface relaxation of the Al atom into the following O layer. The surface O_s binding to the H⁺ of H₂O relaxes upward compared to the remaining two O; “s” denotes a surface site. In addition, a significant change in surface geometry occurs. The Al-O bonds with a length of 1.70 Å for the clean relaxed surface increased to 1.75 Å upon hydroxylation. The Al-O_sH bond length was found to be 1.89 Å, the O-H and O_s-H bonds were 0.972 Å and 0.985 Å, respectively. The OH group is tilted away from the surface normal by 59°, and the H of the O_s-H group is oriented toward one of the surface O atoms. A similar tilting behaviour has been observed in case of methanol⁵⁴ and phenol¹⁶ adsorption onto the (0001) surface of α -Al₂O₃.

The vibrational frequencies of the two distinct O-H stretching modes are computed to be 3917 cm⁻¹ for the OH on top of the Al adsorption site and 3679 cm⁻¹ for the O_sH vibrations. The difference in wavenumbers of 238 cm⁻¹ is in good agreement to that of 225 cm⁻¹ reported by Ranea *et al.*²³.

Compared to the 1-2 dissociation, the 1-4 dissociation of water (a representation of both is presented in Figure 2) was found less stable, in agreement with previous reports^{22, 23}. The computed adsorption energies are 1.27 eV and 1.53 eV for the 1-4 and 1-2 dissociation of

water at 50 % coverage, respectively. Furthermore, we note the previously reported²² large inward relaxation of the free Al adsorption site bound to the O₅H in the 1-4 configuration, which can also be seen in Figure 2D. A less pronounced but similar behaviour is seen in case of the 1-2 dissociation. In the following, we will refer to all adsorption sites in a 1-4 environment to be in 1-4 configuration.

Experimental works conducted on α -Al₂O₃(0001) single crystals by means of Fourier transform infrared spectroscopy (FTIR)^{24, 55} and sum-frequency vibrational spectroscopy (SFVS)⁵⁶ showed the existence of surface hydroxyl as well as of ordered molecularly adsorbed water⁵⁵. SFVS measurements identified two main features at 3700 cm⁻¹ and 3430 cm⁻¹. These peaks are attributed to OH species based on isotope-substitution experiments. The strong peak at 3700 cm⁻¹ assigned to O₅-H vibrations is close to the computed value of 3679 cm⁻¹ in this study. The feature observed at 3430 cm⁻¹, not observed in this work; was assigned to bonded OH stretches of adsorbed water molecules^{24, 55}.

To further investigate the effect of dissociatively adsorbed water, the coverage of 25 %, 50 %, 75 % and 100 % were analysed with respect to surface relaxation and vibrational modes. We will limit our focus of the 50 % and 75 % coverage to two cases exhibiting different structural arrangements (Figure 3 and Figure 4). In case of 50% coverage, the 1-2 dissociation of water is investigated with respect to the 1-4 configuration of the free adsorption site (*parallel arrangement*) and the OH occupied Al adsorption site (*linear arrangement*) (Figure 3). A linear arrangement of two dissociated water molecules causes both adsorption sites to inflict 1-4 configuration upon each other (Figure 4). This assumes the initial 1-2 dissociation of water takes place at the Al_{2S} and O_{2S} adsorption sites, Figure 5. The OH and H of the second dissociated water molecule are on top of the Al_{4S} and the O_{4S} site, respectively. Therefore, one finds the Al_{4S} site in 1-4 configuration with respect to the O_{2S} site as it finds itself across a 6-fold ring (blue). Also, the Al_{2S} site is in 1-4 configuration with respect to the O_{4S} site. In case of a parallel arrangement only the empty Al adsorption site is in 1-4 configuration.

In the case of surface hydroxylation of 75% two models were considered. The first by adopting the 1-4 configuration (*linear*) with respect to the occupied Al adsorption sites of the 50% coverage and adding one dissociated water molecule to the surface as presented in Figure 4A. In the second configuration all water molecules were placed in an arrangement which avoids 1-4 configuration to any occupied Al adsorption site (Figure 4B). This configuration causes the empty adsorption site to be in 1-4 configuration with respect to the dissociative adsorption of water. This is illustrated using a (3 x 3) super cell in Figure 6 where

8

H is bound to the O_S sites labelled as O_{2S} , O_{3S} , and O_{4S} . Therefore, causing the Al_{1S} adsorption site to be in 1-4 configuration with respect to all remaining Al adsorption sites.

Some of the changes upon the coverage-dependent adsorption of dissociated water onto α - $Al_2O_3(0001)$ are listed in Table 2. Upon an increase in surface hydroxylation, negligible change in the O_S -H and O-H distances is observed. While changes are seen with respect to the adsorption energy, for Al-OH bond length, O_S -H and O-H vibration there is no clear pattern with respect to an increase in surface hydroxylation. The most stable configuration is a coverage of 75 %, inflicting a 1-4 configuration to the free adsorption site. The increase in adsorption energy compared to the 25 % surface hydroxylation can be linked to structural relaxation. The lateral relaxation of the investigated surfaces was studied in details (see Table SM2 and Table SM3 for more detail). The largest upward movement of the occupied Al adsorption sites is connected to the deepest relaxation of the free adsorption site into the bulk of the surface.

Comparing these findings to our previous study of the coverage-dependent CO adsorption²⁶ where a linear increase in adsorption energy with decreasing coverage was noted, we found that such a trend is offset by adsorption in 1-4 configuration, creating two different adsorption environments. Plotting the adsorption energy of dissociated water versus coverage, the influence of the 1-4 configuration becomes evident (Figure 7). This arrangement, of the 1-4 configuration, has a stabilising effect as shown in the case of the 75 % when free adsorption sites are in that configuration, while it is destabilising when inflicted upon an occupied adsorption sites.

To further study the adsorbate-substrate interaction the DOS and local density of states (LDOS) plots were calculated from the (1 x 1) surface representing the fully hydroxylated surface. Figure 8 presents the DOS of the clean and fully hydroxylated (1 x 1) surfaces as well as the free water molecule. Figure 9 shows the LDOS plots of surface atoms at the relaxed surface with and without H_2O . The adsorption of water causes, in general, an increased population of the lower lying surface states with respect to the Al and O surface states (Figure 9). A down shift of all occupied orbitals is seen – Table 3. The unoccupied $4a_1$ orbitals remain unchanged. The OH group on top of the surface Al can be identified by an increase in the peak formation consisting of Al 3s and 3p contribution ranging from -5.0 eV to -7.7 eV, and -

1.3 eV (Figure 9A and 9B). The bonding of H to O_S is seen by the formation of a peak at -8.1 eV and -20.6 eV in the LDOS representing the O_S surface states shown in Figure 9C, and Figure 9D.

3.5. CO adsorption onto the hydroxylated (0001) surface of α -Al₂O₃

The CO adsorption onto the hydroxylated surface was modelled by placing the CO molecule perpendicular (with the C of CO facing the surface) on top of an Al adsorption site. The effects of two coverage-dependent adsorption behaviours were examined. In the first case, the coverage of CO molecules adsorbed to a surface exhibiting a pre-existing water coverage of 25 % was changed, whereas in the second case, the CO coverage was kept constant at 25 % on surfaces exhibiting a 25 %, 50 % and 75 % hydroxylation.

The structural and vibrational properties listed in Table 4 show that the adsorption of one CO molecule to a 25% pre-hydroxylated surface is most stable. The adsorption of CO onto an Al adsorption site in 1-4 configuration yields a much weaker binding of CO; 0.44 eV (see Table SM4). Since this surface represents CO coverage of 25 % with one dissociated water molecule, the surface has a total coverage of 50 % with respect to the Al adsorption sites. Therefore, it is worth to compare CO adsorption behaviour at a hydroxylated surface to those of the dry surfaces exhibiting 25 % and 50 % CO coverage (see Table SM1 and Table 4). The CO adsorption energy of 0.57 eV on the hydroxylated surface is slightly stronger than that of 0.52 eV and 0.48 eV on the dry surface with CO coverage of 25 % and 50 %, respectively. The vibrational frequency and the CO bond distance are very close to those of the dry surface representing at 25% coverage, but differ significantly from those of a 50% CO coverage.

3.5.1. Increasing the CO coverage on the hydroxylated surface

The coverage-dependent adsorption of CO was investigated implying a (2 x 2) surface preoccupied by one dissociated water molecule. Thus leaving the Al_{4S} site in 1-4 configuration, with respect to Figure 10. The increase in CO coverage is modelled by occupying subsequently the Al adsorption sites Al_{3S}, Al_{1S}, and Al_{4S}, as shown in Figure 10.

An increase in the CO bond length ranging from 1.148 Å to 1.152 Å is noted, still lower than that of 1.154 Å for the free CO molecule. Associated with the increase in the CO bond length is a decrease in CO wavenumbers from 2225 cm⁻¹ to 2201 cm⁻¹ and a decrease in the CO binding energy from 0.57 eV to 0.43 eV. The O-H bond length remains unaffected, although a decrease in the OH vibrations from 3936 cm⁻¹ to 3924 cm⁻¹ with the increasing of the CO

coverage is seen. At a CO coverage of 75 %, significant structural changes are observed. These changes are very likely to result from the 1-4 configuration of the free Al_{4S} adsorption site where the final CO molecules was added. The most noticeable is the decrease in the interlayer distance of the Al_{2S} site bound to the OH fragment from 0.748 Å to 0.706 Å upon an increase in CO coverage. This is accompanied by a steady relaxation of the O_S site binding to the H into the top O layer. CO adsorption to the Al_{3S} also shows a trend of decreasing interlayer distances upon an increase in CO adsorption. A similar relaxation pattern was noted for the coverage-dependent CO adsorption onto the dry surface. Comparing the results of a surface with a hydroxylation of 25 % in the presence of one CO molecule to a 25 % surface hydroxylation in the absence of CO, we note the following three observations: 1. An enhanced relaxation with respect to the relaxation of the Al_{2S} site. 2. A further decent of the Al_{4S} site in the bulk. 3. The O_S site binding to the H reveals a slightly shorter interlayer distance to the following O layer.

3.5.2. Effect of degree of hydroxylation on CO adsorption.

CO adsorption onto an increasingly hydroxylated surface (25%, 50% and 75%) is presented in (Figure 11 and Figure SM2). The cases investigated represent the most stable hydroxylated surfaces, with the exception of the 75% surface hydroxylation. In this case, both previously examined surface arrangements were being considered, see Figure 4. The adsorption of CO was found to be stable for all investigated coverage with the exception of the 75% surface hydroxylation, as presented in Figure 4B. Since the free Al adsorption finds itself far below the surface plane, thus no CO adsorption is plausible.

Table 5-7 present the structural and vibrational properties of CO and water with increasing hydroxylation. With the exception of the Al-C bond length increasing from 2.161 Å to 2.177 Å, the remaining C-O, Al-OH, O-H and O_S-H bond distances are little affected. The O_S-H vibration belonging to the Al-OH site inflicting 1-4 configuration upon the CO adsorption site (which is the free Al adsorption site in Figure 4A) shifted to higher wavenumbers compared to their counterpart acting in the same way on a free or OH occupied Al adsorption site. Also an increase in the CO vibrational frequency to approximately 2240 cm⁻¹ upon surface hydroxylation at and above 50% is noted, while the CO adsorption energy was found to decrease with increasing surface hydroxylation.

It is clear from this work that the main effect on the adsorption energy of CO on α -Al₂O₃ (0001) surface is structural variations and not electronic. This is in large due to the initial strong relaxation of the last atomic layer, whereby the Al atoms relax downwards from bulk position due to strong electrostatic bonds with oxygen atoms. The adsorption of CO or water partially revert this process locally. Thus any adsorption adjacent to this is largely affected by surface reconstruction. Unlike the case of TiO₂, for example⁵⁷ (where lateral effect takes place), these large reconstructions allow for a restricted local environment where the second adsorption take place, as seen for example in figure 2 and tables 5 and 6 where the 1,2 configuration allows for a stronger bonding when compared to the 1,4 configuration. One of the implications of these observations may be considered in the case of the adsorption of CO on M/ α -Al₂O₃ (0001) surface. Because of the weak interaction of CO on α -Al₂O₃ (0001) surface and the absence of lateral attractive effect CO would preferentially bind to the metal at low coverage. In a work focusing on the adsorption of CO on α -Al₂O₃ (0001) and on Pd and Ag deposited on α -Al₂O₃ (0001) it was found that adsorption is preferred on the metal and not on the surface site adjacent to the metal⁵⁸. This was not due to the larger adsorption energy of CO on Ag deposited on α -Al₂O₃ (0001) (E_a CO on Ag/ α -Al₂O₃ (0001) = 0.6 eV and E_a CO on α -Al₂O₃ (0001) = 0.53 eV) but mainly because of structural effect. Similar observations related to energy differences were found for Au/Al₂O₃ although with subtle differences⁵⁹. CO preferentially adsorbs on Au/ α -Al₂O₃ (0001) but may adsorb on Al sites in the case of Au/Al₂O₃ (clusters – amorphous).

4. Conclusions

We have investigated the coverage-dependent 1-2 dissociative adsorption of water onto the (0001) surface of Al₂O₃ to study the coverage-dependent CO adsorption. Hydroxylation of the clean surface takes place via adsorption of the OH group on top the Al adsorption site, while the H binds to one of the three nearest O neighbours. An adsorption site in 1-4 configuration is characterised by its position across a six-fold ring with respect to the H of water binding to a surface O next to the Al-OH adsorption site. This arrangement causes the Al site to relax deep into the surface, therefore, being less available for further adsorption. This was verified by the fact that any adsorption taking place at this site is found to be less stable. Therefore, we concluded the most stable surfaces to be those who inflict 1-4 configuration only onto a free adsorption site. The surface exhibiting a surface hydroxylation of 75 % is reported to be the most stable one.

CO adsorption onto the hydroxylated surface shows a rather complex adsorption behaviour. CO adsorption was studied with respect to increasing coverage upon a pre-hydroxylated surface. The most stable CO adsorption is found on a surface exhibiting a hydroxylation of 25% at a CO coverage of 25%, which resulted in a stronger CO adsorption energy compared to the same coverage on the clean surface. With increasing CO coverage, a decreasing CO adsorption energy coupled with a decrease in the CO vibrational frequency was noted. CO adsorption onto surfaces exhibiting a hydroxylation of 25%, 50% and 75% was found to be stable, with the exception of the surface exhibiting the most stable hydroxylation (75%). An increase in surface hydroxylation also resulted in a reduced CO adsorption energy. However, an increase in the CO wavenumber was noted for surface hydroxylation at and above 50%.

5. References

1. V. E. Henrich and P. A. Cox, *The Surface Science of Metal Oxides*, Cambridge University Press, New York, 1994.
2. F. Pompeo, D. Gazzoli and N. N. Nichio, *Mater. Lett.*, 2009, 63, 477.
3. M. S. Moreno, F. Wang, M. Malac, T. Kasama, C. E. Gigola, I. Costilla and M. D. Sánchez, *J. Appl. Phys.*, 2009, 105, 083531.
4. J. Ahn and J. W. Rabalais, *Surf. Sci.*, 1997, 388, 121.
5. J. Toofan and P. R. Watson, *Surf. Sci.*, 1998, 401, 162.
6. I. Manassidis and M. J. Gillan, *J. Am. Ceram. Soc.*, 1994, 77, 335.
7. M. Gautier-Soyer, F. Jollet and C. Noguera, *Surf. Sci.*, 1996, 352, 755.
8. Z. Łodziana and J. K. Nørskov, *J. Chem. Phys.*, 2001, 115, 11261.
9. T. Worren, K. Højrup Hansen, E. Lægsgaard, F. Besenbacher and I. Stensgaard, *Surf. Sci.*, 2001, 477, 8.
10. J. R. B. Gomes, Z. Łodziana and F. Illas, *J. Phys. Chem. B*, 2003, 107, 6411.
11. C. Zhou, J. Wu, T. J. D. Kumar, N. Balakrishnan, R. C. Forrey and H. Cheng, *J. Phys. Chem. C*, 2007, 111, 13786.
12. J. A. Keller, N. Chengyu, K. Shepherd, D. R. Jennison and A. Bogicevic, *Surf. Sci.*, 2000, 446, 76.
13. C. Niu, K. Shepherd, D. Martini, J. Tong, J. A. Kelber, D. R. Jennison and A. Bogicevic, *Surf. Sci.*, 2000, 465, 163.
14. S. Alavi, D. C. Sorescu and D. L. Thompson, *J. Phys. Chem. B*, 2003, 107, 186.
15. J. W. Elam, C. E. Nelson, M. A. Tolbert and S. M. George, *Surf. Sci.*, 2000, 450, 64.
16. S. D. Chakarova-Käck, Ø. Borck, E. Schröder and B. I. Lundqvist, *Phys. Rev. B*, 2006, 74, 155402.
17. D. C. Sorescu, J. A. Boatz and D. L. Thompson, *J. Phys. Chem. B*, 2005, 109, 1451.
18. V. A. Ranea, W. F. Schneider and I. Carmichael, *Surf. Sci.*, 2008, 602, 268.
19. J. M. McHale, A. Auroux, A. J. Perrotta and A. Navrotsky, *Science*, 1997, 277, 788.
20. J. W. Elam, C. E. Nelson, M. A. Cameron, M. A. Tolbert and S. M. George, *J. Phys. Chem. B*, 1998, 102, 7008.
21. V. Shapovalov and T. N. Truong, *J. Phys. Chem. B*, 2000, 104, 9859.

22. K. C. Hass, W. F. Schneider, A. Curioni and W. Andreoni, *J. Phys. Chem. B*, 2000, 104, 5527.
23. V. A. Ranea, I. Carmichael and W. F. Schneider, *J. Chem. Phys. C*, 2009, 113, 2149.
24. A. C. Thomas and H. H. Richardson, *J. Phys. Chem. C*, 2008, 112, 20033.
25. M. Casarin, C. Maccato and A. Vittadini, *Inorg. Chem.*, 2000, 39, 5232.
26. C. Rohmann, J. B. Metson and H. Idriss, *Surf. Sci.*, 2011, 605, 1694.
27. A. Soon, T. Söhnle and H. Idriss, *Surf. Sci.*, 2005, 579, 131.
28. G. Pacchioni, G. Cogliandro and P. S. Bagus, *Surf. Sci.*, 1991, 255, 344.
29. C. Müller, C. Freysoldt, M. Baudin and K. Hermansson, *Chem. Phys.*, 2005, 318, 180.
30. G. Pacchioni, A. M. Ferrari and P. S. Bagus, *Surf. Sci.*, 1996, 350, 159.
31. M. Kunat, F. Traeger, D. Silber, H. Qiu, Y. Wang, A. C. van Veen, C. Wöll, P. Kowalski, B. Meyer, C. Hättig and D. Marx, *J. Chem. Phys.*, 2009, 130, 144703.
32. C. Rohmann, Y. Wang, M. Muhler, J. Metson, H. Idriss and C. Wöll, *Chem. Phys. Lett.*, 2008, 460, 10.
33. A. Zecchina, D. Scarano, S. Bordiga, G. Spoto and C. Lamberti, *Adv. Catal.*, 2001, 46, 265.
34. K. Hadjiivanov, J. Lamotte and J.-C. Lavalley, *Langmuir*, 1997, 13, 3374.
35. L. Ferretto and A. Glisenti, *Chem. Mater.*, 2003, 15, 1181.
36. H. Idriss, *Platin. Met. Rev.*, 2004, 48, 105.
37. B. E. Hayden and A. M. Bradshaw, *Surf. Sci.*, 1983, 125, 787.
38. G. L. Griffin and J. T. Yates Jr., *J. Chem. Phys.*, 1982, 77, 3751.
39. A. Zecchina, E. E. Platero and O. C. Areán, *J. Catal.*, 1987, 107, 244.
40. T. H. Ballinger and J. T. Yates Jr., *Langmuir*, 1991, 13, 3041.
41. E. N. Gribov, O. Zavorotynska, G. Agostini, J. G. Vitillo, G. Ricchiardi, G. Spoto and A. Zecchina, *Phys. Chem. Chem. Phys.*, 2010, 12, 6474.
42. S. J. Clark, M. D. Segall, C. J. Pickard, P. J. Hasnip, M. J. Probert, K. Refson and M. C. Payne, *Z. Kristallogr.*, 2005, 220, 567.
43. J. P. Perdew, K. Burke and M. Ernzerhof, *Phys. Rev. Lett.*, 1996, 77, 3865.
44. H. J. Monkhorst and J. D. Pack, *Phys. Rev. B*, 1976, 13, 5188.
45. K. Laasonen, A. Pasquarello, R. Car, C. Lee and D. Vanderbilt, *Phys. Rev. B*, 1993, 47, 10142.
46. B. G. Pfrommer, M. Côté, S. G. Louie and M. L. Cohen, *J. Comput. Phys.*, 1997, 131, 233.
47. B. Hinnemann and E. A. Carter, *J. Phys. Chem. C*, 2007, 111, 7105.
48. L. Ouyang and W.-Y. Ching, *J. Am. Ceram. Soc.*, 2001, 84, 801.
49. J. L. Dunham, *Phys. Rev.*, 1932, 41, 721.
50. C. G. Elles, C. A. Rivera, Y. Zhang, P. A. Pieniazek and S. E. Bradforth, *J. Chem. Phys.*, 2009, 130, 084501.
51. A. R. Hoy and P. R. Bunker, *J. Mol. Spectr.*, 1979, 74, 1.
52. C. Verdozzi, D. R. Jennison, P. A. Schultz and M. P. Sears, *Phys. Rev. Lett.*, 1999, 82, 799.
53. J. Carrasco, J. R. B. Gomes and F. Illas, *Phys. Rev. B*, 2004, 69, 064116.
54. Ø. Borck and E. Schröder, *J. Phys. Condens. Matter*, 2006, 18, 1.
55. H. A. Al-Abadleh and V. H. Grassian, *Langmuir*, 2003, 19, 341.
56. L. Zhang, C. Tian, G. A. Waychunas and R. Y. Shen, *J. Am. Chem. Soc.*, 2008, 130, 7686.
57. J. Scaranto and S. Giorgianni, *Molecular Physics*, 2009, 107, 1997.
58. J. Blomqvist, L. Lehmany, P. Salo, *Phys. Status Solidi B*, 2012, 249, 1046.
59. E.M. Fernández and L.C. Balbás, *J. Phys. Chem. B*, 2006, 110, 10449.

14

60. E.M. Fernández, R.I. Eglitis, G. Borstel, L.C. Balbás, *Computational Materials Science* 2007, 39, 587.

Figures

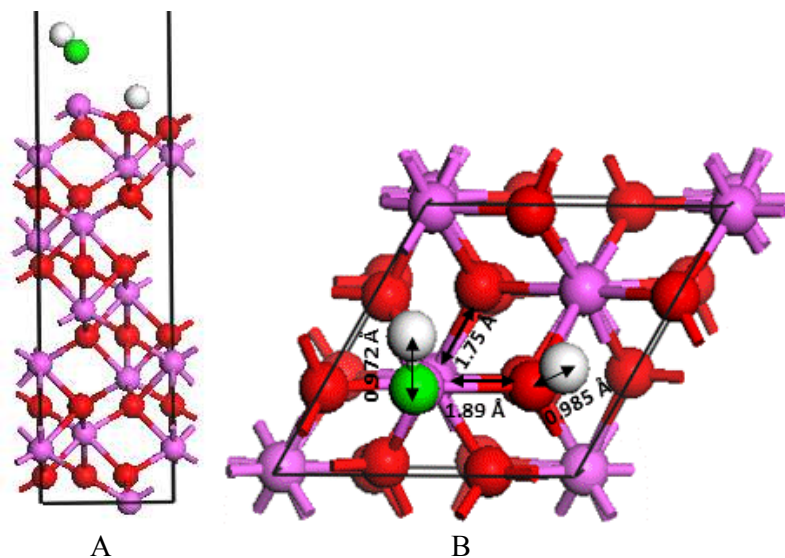
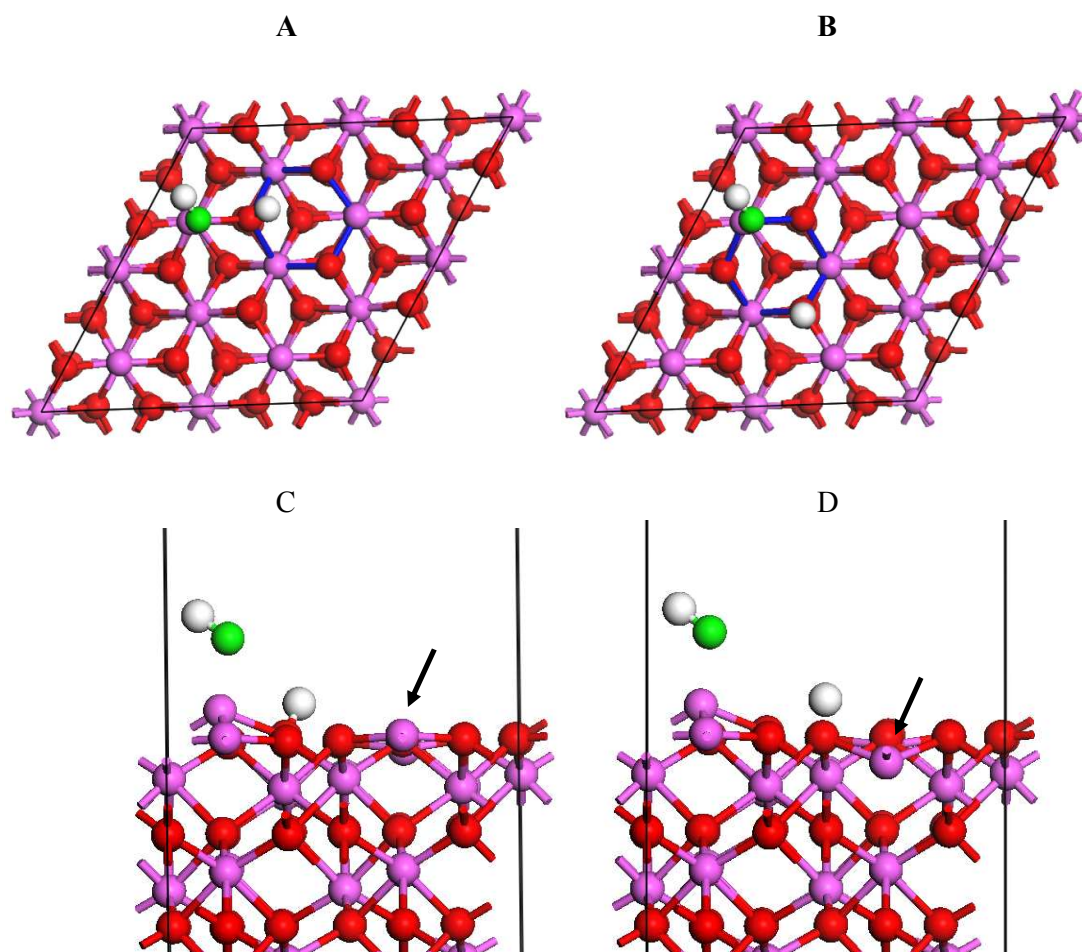


Figure 1:

(A) 1-2 water dissociation representing the full coverage on the (1 x 1) surface of α - $\text{Al}_2\text{O}_3(0001)$ in side view and
(B) top view. Al and O atoms are in purple and red, respectively, while H and O atoms of H_2O are in light grey and green, respectively.

16

**Figure 2:**

The (2×2) $\text{Al}_2\text{O}_3(0001)$ surface representing (A) the 1-2 and (B) 1-4 dissociation of water. (A) and (B) Top views showing the H to adsorb in 1-2 configuration on one of the nearest neighbour O atoms, while the H in 1-4 configuration adsorbs across a six-fold ring (blue) with respect to the Al adsorption site. (C) and (D) Side views of the 1-2 and 1-4 dissociation of water.

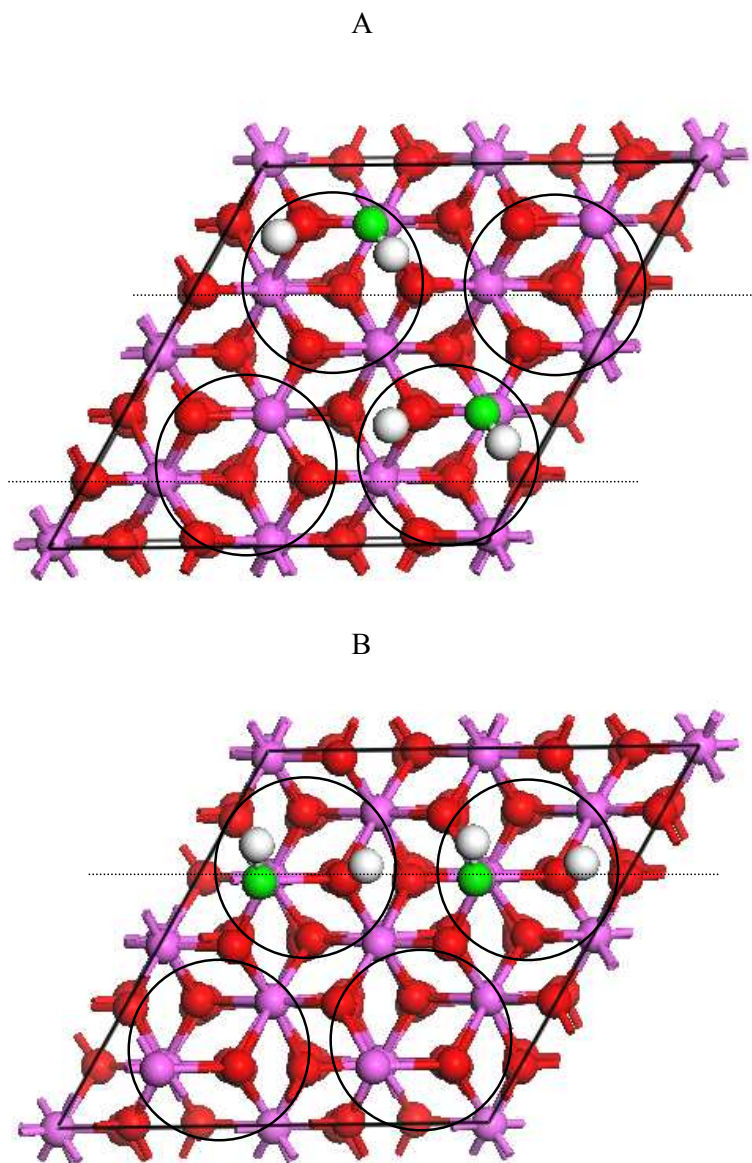


Figure 3:

A top view of dissociative water adsorption at coverage of 50 % on to the (2×2) $\text{Al}_2\text{O}_3(0001)$ surface in a parallel (A) and linear (B) configuration. The circles are a guide to see the available pairs for the dissociative adsorption. In each surface there are four circles for the four possible water dissociative adsorptions.

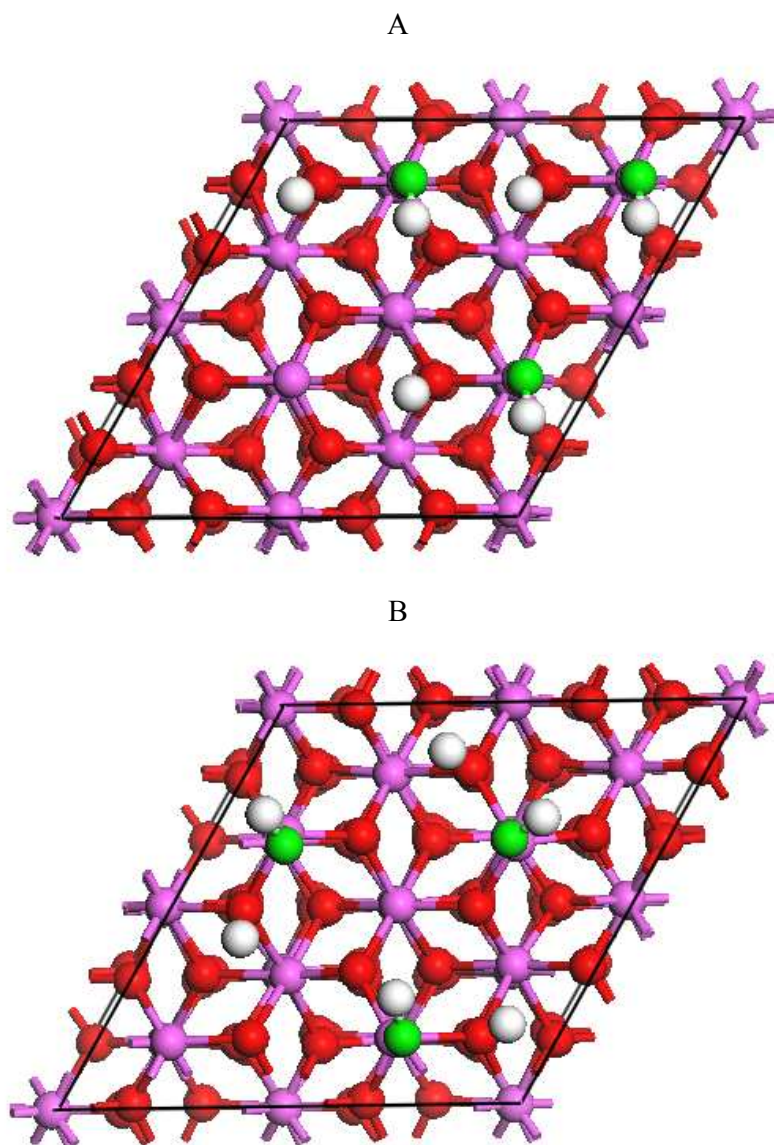
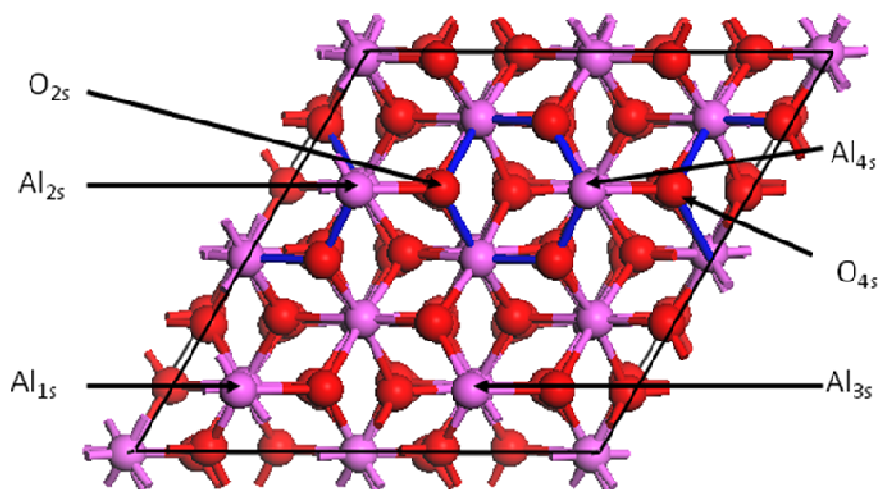


Figure 4:

A top view of two (2 x 2) surfaces exhibiting a 75 % surface hydroxylation. (A) The dissociative adsorption of water inflicting the 1-4 configuration on two out of three Al adsorption sites is presented on top. (B) The dissociative adsorption of water in an arrangement where none of the occupied adsorption sites is in the 1-4 configuration.

**Figure 5:**

The (2×2) α - $\text{Al}_2\text{O}_3(0001)$ surface. The four Al adsorption sites and the 6-fold rings (blue) of the Al_{2s} and Al_{4s} adsorption sites are shown. The O_{2s} and O_{4s} adsorption sites are shown to represent 1-2 configuration/1-4 configuration with respect to the $\text{Al}_{2s}/\text{Al}_{4s}$ adsorption sites. The subscript numbers of the O adsorption sites indicate the nearest neighbour Al adsorption site.

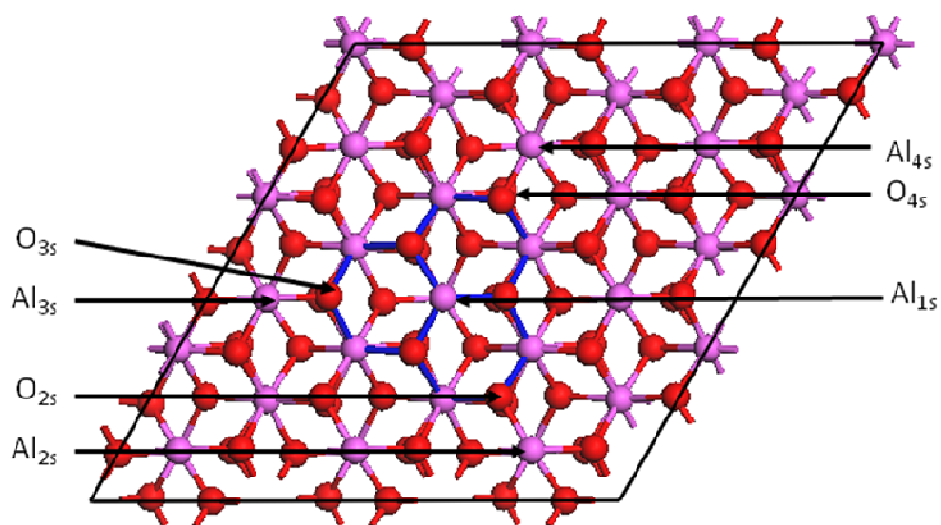
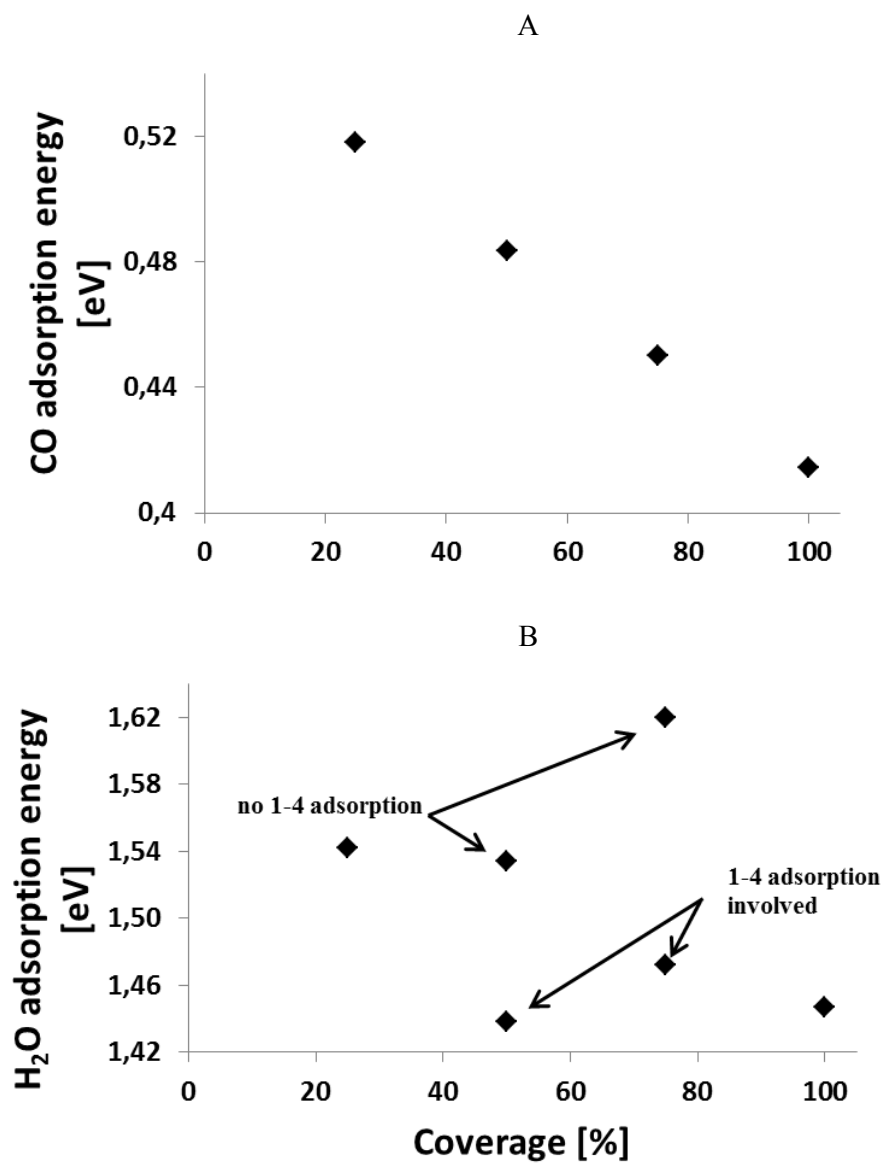
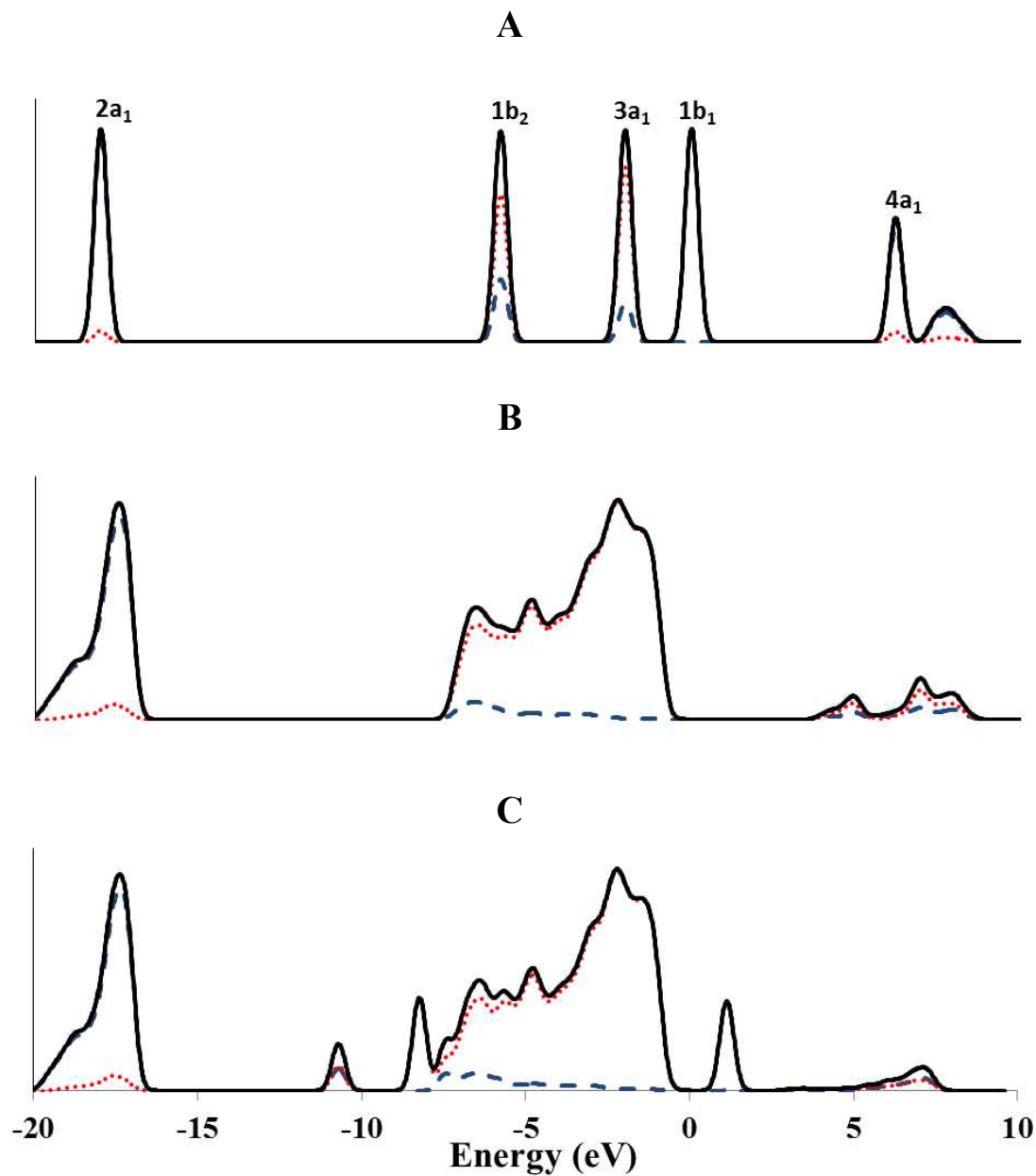


Figure 6:

A (3×3) surface of bare α - $\text{Al}_2\text{O}_3(0001)$. The four Al adsorption sites and the three O adsorption sites inflicting 1-4 arrangement onto the Al_{1s} site by being placed across a 6-fold (blue) are shown.

**Figure 7:**

- (A) Coverage dependence of CO adsorption onto $\alpha\text{-Al}_2\text{O}_3(0001)$.
(B) Coverage dependence of 1-2 dissociative water adsorption onto $\alpha\text{-Al}_2\text{O}_3(0001)$.

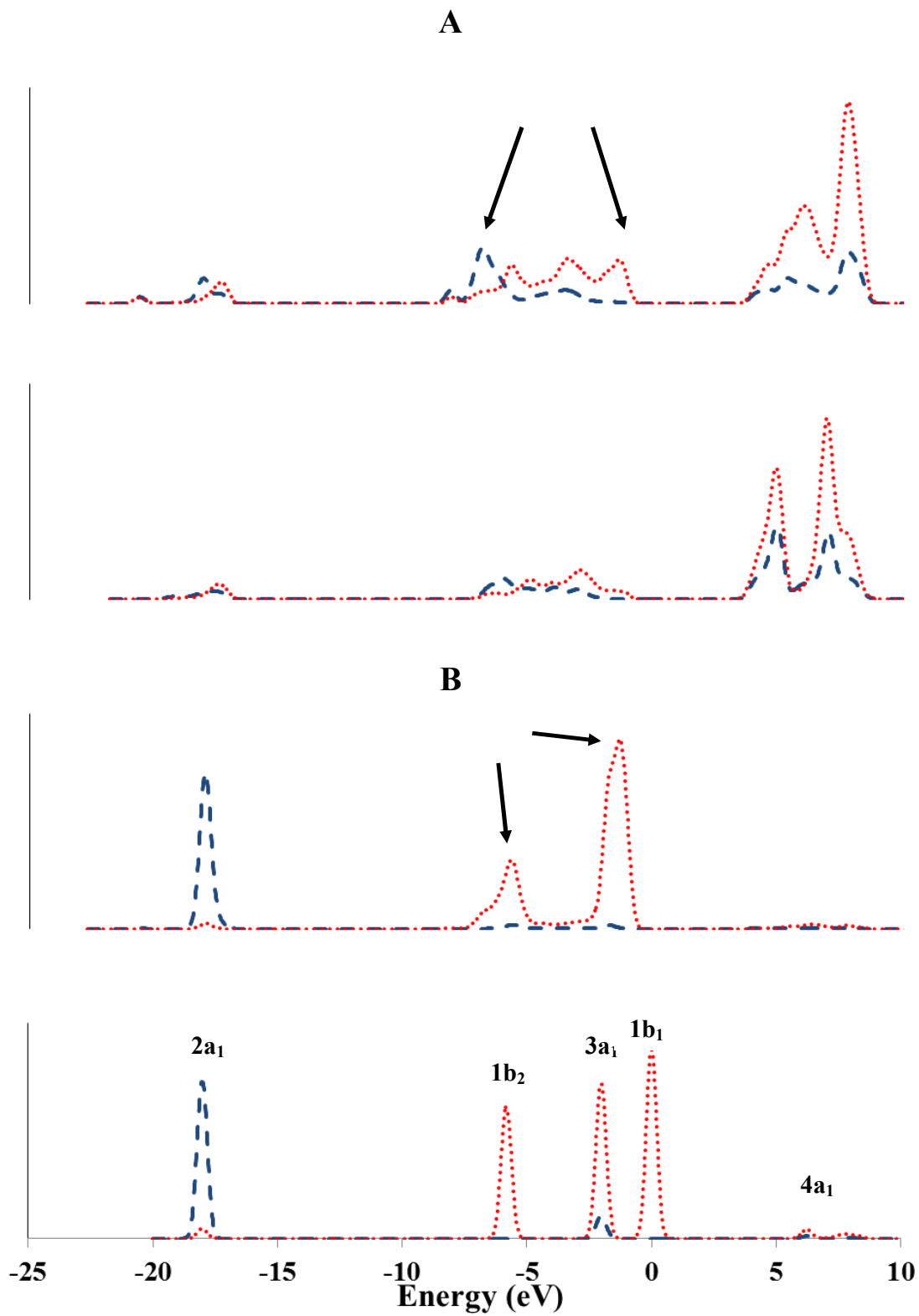
**Figure 8:**

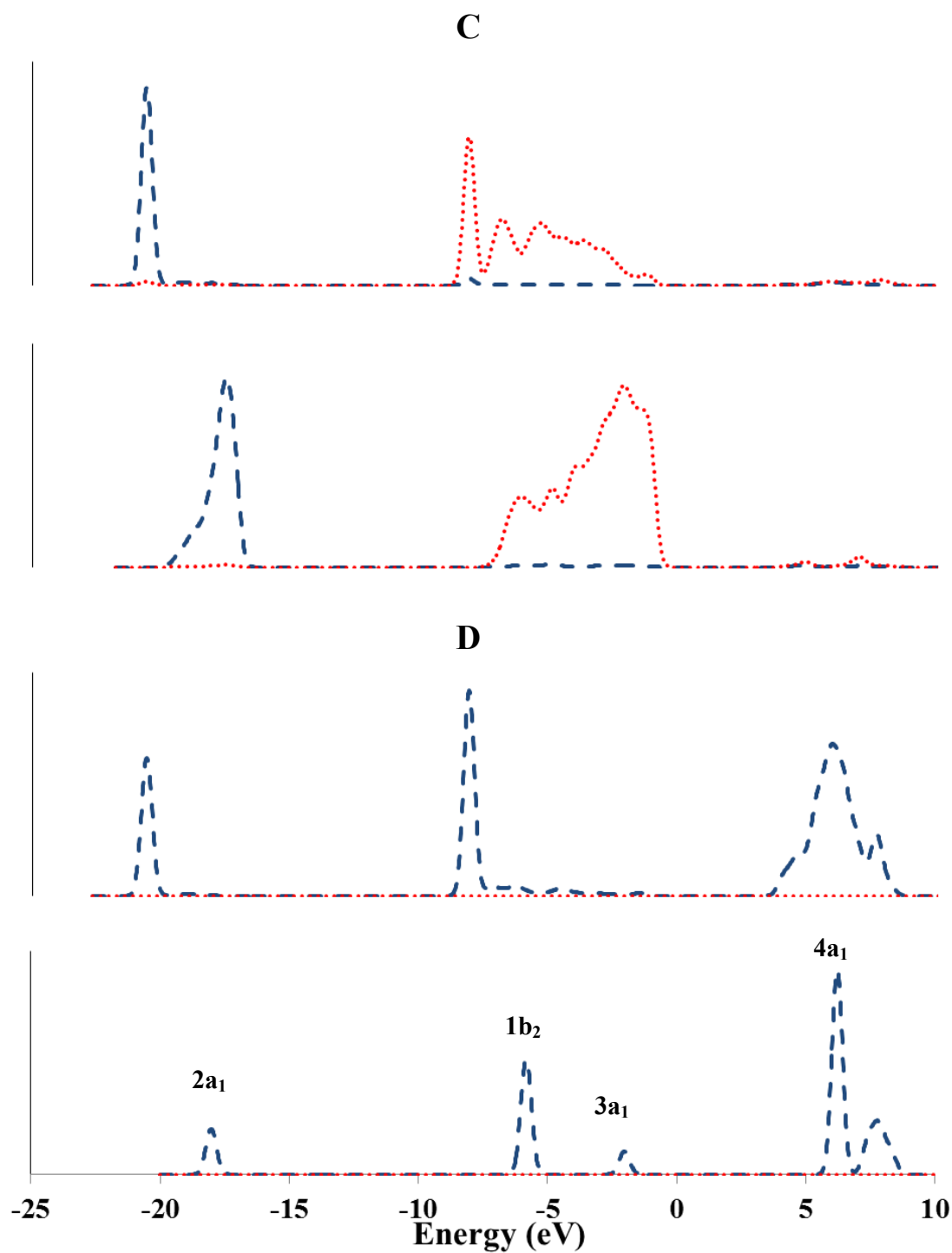
(A) DOS of the free H₂O molecule.

(B) LDOS (surface states only) of the clean α -Al₂O₃(0001) surface.

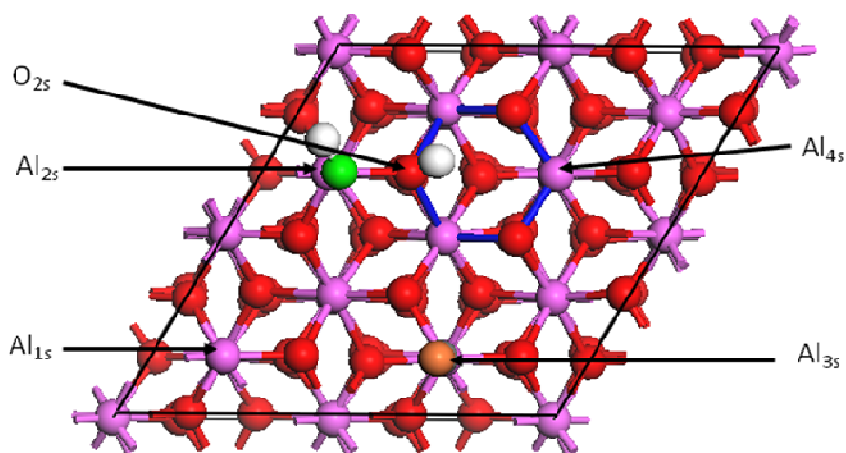
(C) LDOS (surface states only) of H₂O adsorption onto the α -Al₂O₃(0001) surface.

Dashed and dotted lines represent s and p contributions, respectively, while solid lines are the sum of s and p contributions. The Fermi level is at 0.0 eV.



**Figure 9:**

- (A) LDOS plots of Al surface states of H₂O/ α -Al₂O₃(0001) and α -Al₂O₃(0001).
 (B) LDOS plots of O (O-H) surface states of H₂O/ α -Al₂O₃(0001) and O of H₂O(g).
 (C) LDOS plots of O of O_s-H states of H₂O/ α -Al₂O₃(0001) and O of α -Al₂O₃(0001).
 (D) LDOS plots of H of O_s-H states of H₂O/ α -Al₂O₃(0001) and H of H₂O (g).
 Dashed and dotted lines are s and p contributions, respectively. The Fermi level is at 0.0 eV.

**Figure 10:**

The (2 × 2) surface showing 1-2 dissociation of water at the Al_{2s} and O_{2s} sites, whereas CO adsorption takes place at the Al_{3s} site. For clarity, the O atom of CO is in orange. The empty adsorption Al_{4s} site is located across a 6-membered ring, therefore being in 1-4 configuration.

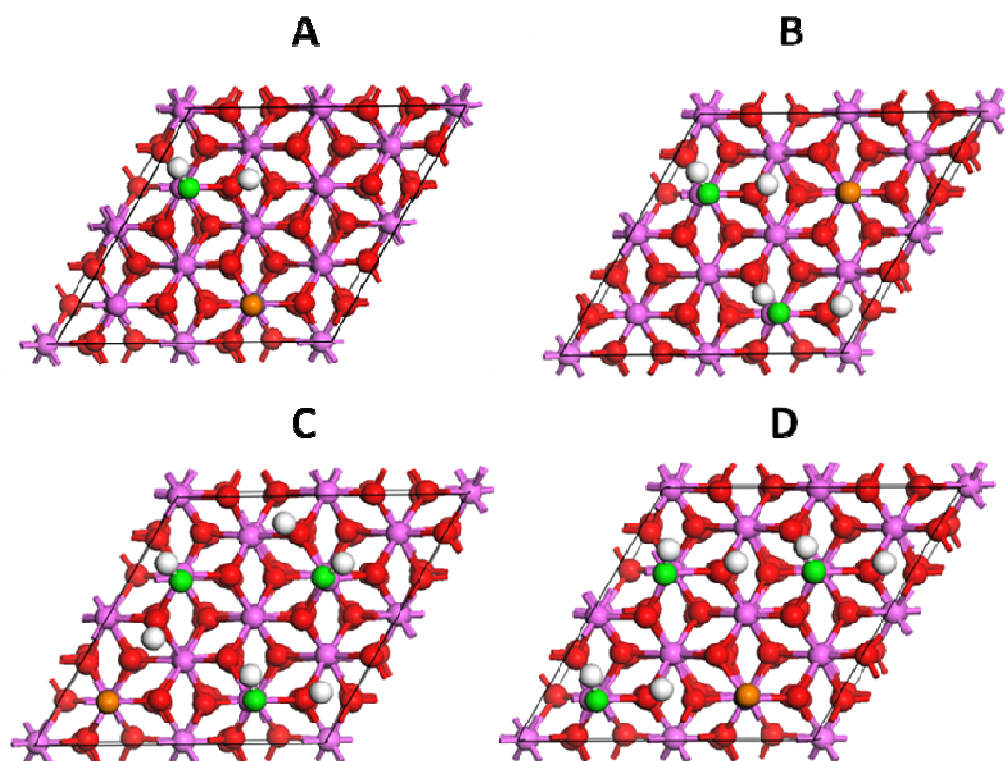


Figure 11:

- (a) 25 % hydroxylation, 1-4 inflicted on the free Al adsorption site.
 - (b) 50 % hydroxylation, 1-4 inflicted on CO and the free adsorption site.
 - (c) 75 % hydroxylation, structure A.
 - (d) 75 % hydroxylation, structure B.
- All results are on the 25% CO coverage.

Tables

Table 1:

Comparison of layer relaxation of the fully hydroxylated (1 × 1) surface along the z-axis in % and Å with respect to the unrelaxed structure.

	Clean surface (%)	Clean surface (Å)	Hydroxylated Surface (%)	Hydroxylated surface (Å)
Al ₁ /O ₂	-89.98	-0.760	-14.64 (-13) ^[a]	-0.124 (-0.11) ^[a]
O ₂ /Al ₃	+3.19	+0.027	-0.72	-0.006
Al ₃ /Al ₄	-45.11	-0.225	-31.98	-0.160
Al ₄ /O ₅	+20.16	+0.170	+10.34	+0.087
O ₅ /Al ₆	+6.23	+0.053	+0.43	+0.004

Negative signs indicate the movement of two layers towards each other, while positive ones indicate that apart from each other. The subscript number indicates the layer number starting from the surface. [a] From reference²²

Table 2:

Structural and vibrational properties of adsorbed H₂O onto α -Al₂O₃(0001). Sections shaded grey present water adsorption onto an Al adsorption site in 1-4 configuration.

surface	(2 x 2)	(2 x 2)	(1 x 2)	(2 x 2)	(2 x 2)	(1 x 1)
coverage [%]	25	50	50	75	75	100
r_{Al-OH} [Å]	1.725	1.721 ¹	1.723	1.716 ¹	1.718 ¹	1.720
r_{Os-H} [Å]	0.971	0.971 ¹	0.971	0.971 ¹	0.971 ¹	0.972
ν_{Os-H} [cm ⁻¹]	3707	3712	3648	3692	3670	3679
ν_{O-H} [cm ⁻¹]	3934	3918	3927	3928	3929	3917
Adsorption energy [eV]	1.54	1.53	1.44	1.62	1.47	1.45

¹ An average value is presented.

For comparison the adsorption energy of H₂O using un-relaxed Hartree–Fock calculation of the CRYSTAL code gave adsorption energy (binding energy) = 1.31 eV, 1.53 eV, and 1.29 eV, for the molecular, 1-2, and 1-4 configuration, respectively⁶⁰. This to be compared to 1.01 eV, 1.44 eV, and 1.41 eV for the three modes using CPMD with GGA/BLYP²²

Table 3:

Energy level in eV for H₂O orbitals for free and adsorbed water on α -Al₂O₃(0001). Δ is the difference in eV.

Orbital	Free H ₂ O	H ₂ O/ α -Al ₂ O ₃	Δ
4a ₁	+6.2	+6.2	+0.0
1b ₁	+0.0	-1.3	-1.3
3a ₁	-2.0	-5.7	-3.7
1b ₂	-5.8	-8.1	-2.3
2a ₁	-18.0	-20.6	-2.6

Table 4:

Structural and vibrational properties of an increased CO coverage to the (2 x 2) surface of α - $\text{Al}_2\text{O}_3(0001)$ exhibiting a water coverage of 25 %.

	2x2	2 x 2	2 x 2	2 x 2	2x2 ³
H ₂ O coverage [%]	25	25	25	25	25
CO coverage [%]	0	25	50	75	75 (1-4)
Total coverage	25	50	75	100	100
r_{C-O} [Å]	--	1.148	1.149 ²	1.151 ²	1.152
r_{Al-C} [Å]	--	2.161	2.157 ²	2.177 ²	2.207
r_{Al-OH} [Å]	1.725	1.731	1.738	1.748	1.748
r_{O-H} [Å]	0.971	0.971	0.971	0.972	0.972
r_{Os-H} [Å]	0.985	0.985	0.984	0.981	0.981
ν_{C-O} [cm ⁻¹]	--	2225	2223 ²	2208 ²	2201
Δ_{C-O} [cm ⁻¹]	--	55	53 ²	38 ²	31
ν_{O-H} [cm ⁻¹]	3934	3936	3927	3924	3924
ν_{Os-H} [cm ⁻¹]	3707	3696	3696	3747	3747
CO adsorption energy [eV]	--	0.57	0.54	0.43	0.43

² An average value of the two equivalent CO molecules is presented.

³ The CO molecule finding itself in the 1-4 configuration with respect to the protonated surface Os.

Only at 75 % CO coverage, the adsorption of one CO molecule takes place in a 1-4 configuration.

Table 5:

Comparison of inter layer distance in Å of different CO coverage at the partially (25 %) hydroxylated surface of α -Al₂O₃(0001).

Inter layer spacing [Å]	Coverage H ₂ O/CO [%]	Al _{1S}	Al _{2S} OH	Al _{3S}	Al _{4S} ⁵
Al ₁ /O ₂	25/0	0.112	0.742	0.125	-0.211
Al ₁ /O ₂	25/25	0.093	0.748	<i>0.364</i>	-0.342
Al ₁ /O ₂	25/50	<i>0.321</i>	0.721	<i>0.324</i>	-0.377
Al ₁ /O ₂	25/75	<i>0.280</i>	0.706	<i>0.290</i>	<i>0.238</i>
O _S /O ₂ ⁴	25/0	0	0.100	0	0
O _S /O ₂ ⁴	25/25	0	0.095	0	0
O _S /O ₂ ⁴	25/50	0	0.087	0	0
O _S /O ₂ ⁴	25/75	0	0.084	0	0

⁴ The relaxation of the protonated O being a nearest neighbour of the indicated Al adsorption site is given.

⁵ The Al_{4S} position finds itself in 1-4 configuration with respect to adsorbed water.

The subscript number indicates the layer number starting from the surface. The bold and italic numbers represent lateral movement induced by OH and CO adsorption respectively. Interlayer distances were computed by averaging over all atoms within one layer. In case of the O_S-H adsorption site the averaging was done with respect to the none protonated O_S counterparts.

Table 6:

Structural and vibrational properties of CO adsorbed to the (2 x 2) surface of Al₂O₃(0001) exhibiting a water coverage of 25 %, 50 %, and 75 %.

	(2 x 2)	(2 x 2) ^{7, 8}	(2 x 2) ⁷	(2 x 2) ^{7, 9}	(2 x 2) ^{7, 8}
H ₂ O coverage [%]	25	50	50	75	75
CO coverage [%]	25	25	25	25	25
Total coverage	50	75	75	100	100
r_{C-O} [Å]	1.148	1.147	1.147	1.147	1.147
r_{Al-C} [Å]	2.161	2.170	2.170	2.177	2.177
r_{Al-OH} [Å]	1.731	1.731	1.729	1.728 ⁶	1.732
r_{O-H} [Å]	0.971	0.972	0.972	0.972 ⁶	0.973
r_{Os-H} [Å]	0.985	0.983	0.985	0.984 ⁶	0.982
ν_{C-O} [cm ⁻¹]	2225	2240	2240	2242	2242
Δ_{C-O} [cm ⁻¹]	55	70	70	72	72
ν_{O-H} [cm ⁻¹]	3936	3914	3910	3921	3914
ν_{Os-H} [cm ⁻¹]	3696	3733	3710	3701	3747
CO adsorption energy [eV]	0.57	0.52	0.52	0.48	0.48

⁶ An average value of the two equivalent H₂O molecules is presented.

⁷ The CO molecule is finding itself in 1-4 configuration, with respect to one adsorbed water molecule.

⁸ Al-OH adsorption site inflicting 1-4 position upon CO adsorption is presented.

⁹ Al-OH adsorption site in 1-4 position is presented.

Table 7:

Comparison of inter layer distance in Å caused by CO adsorption to the (2 x 2) surface of α -Al₂O₃(0001) exhibiting a water coverage of 25 %, 50 % and 75 %.

Inter layer spacing [Å]	Coverage H ₂ O/CO[%]	Al _{1s} ¹¹	Al _{2s} ¹¹	Al _{3s} ¹¹ CO	Al _{4s} ¹¹ Free
Al ₁ /O ₂	25/25	0.093	0.748	<i>0.364</i>	-0.342(1-4)
Al ₁ /O ₂	50/25	0.737	0.732	<i>0.312</i> (1-4)	-0.337(1-4)
Al ₁ /O ₂	75/25	0.681 ^{12,(1-4)}	0.712	<i>0.295</i> (1-4)	--
O _s /O ₂ ¹⁰	25/25	0	0.094 ¹³	0	0
O _s /O ₂ ¹⁰	50/25	0.107 ¹⁴	0.091 ¹³	0	0
O _s /O ₂ ¹⁰	75/25	0.118 ^{12, 14}	0.089 ¹³	0	--

¹⁰ The relaxation of the protonated O being a nearest neighbour of the indicated Al adsorption site is given.

¹¹ The Al adsorption sites presented are being arranged in a way which allows for better comparison of interlayer changes. The subscript numbers are used to distinguish between the different adsorption sites with respect to each other, which is different to the assignment used previously.

¹² An average value of the water dissociation on the Al adsorption sites in 1-4 position is presented.

¹³ The O_s binding to the H inflicting 1-4 configuration to the CO adsorption sites is presented.

¹⁴ O_s being next to an Al in 1-4 arrangement.

The subscript number indicates the layer number starting from the surface. The bold and italic numbers represent lateral movement induced by OH and CO adsorption respectively. Interlayer distances were computed by averaging over all atoms within one layer. In case of the O_s-H adsorption site the averaging was done with respect to the none protonated O_s counterparts. The adsorption sites finding themselves in 1-4 configuration are labelled 1-4.

Supporting Information

**Carbon monoxide adsorption onto hydroxylated
 α -Al₂O₃(0001) surfaces.**

Table SM1:

Structural and vibrational properties of free and adsorbed CO.

	Free CO	2 x 2	2 x 2	2 x 2	1 x 1
Adsorption site	--	Al _{1S}	Al _{1S} and Al _{4S}	Al _{1S} and Al _{3S}	--
coverage [%]	--	25	50	75	100
r_{C-O} [Å]	1.154	1.149	1.150	1.151	1.152
r_{Al-C} [Å]	--	2.148	2.160	2.170	2.183
ν_{C-O} [cm ⁻¹]	2170	2226	2215	2203 ¹⁵	2200
Δ_{C-O} [cm ⁻¹]		56	45	32	30
Adsorption energy [eV]	--	0.52	0.48	0.45	0.42

¹⁵ An average value of the Al_{1S} and Al_{3S} is presented.

Table SM2:

Comparison of inter layer distances in Å of different water coverage is presented for adsorption sites in 1-4 configuration.

Inter layer spacing [Å]	Coverage [%]	Al _{1s}	Al _{2s}	Al _{3s}	Al _{4s}
Al ₁ /O ₂	25	--	--	--	-0.211
Al ₁ /O ₂	50	--	-0.102	--	-0.101
Al ₁ /O ₂ ¹⁶	50	0.683	--	0.683	--
Al ₁ /O ₂ ¹⁷	75	-0.147	0.719	--	0.702
Al ₁ /O ₂ ¹⁸	75	-0.496	--	--	--
Al ₁ /O ₂ ¹⁹	100	0.537	0.537	0.537	0.537
O _s /O ₂ ^{20, 16}	50	0.132	--	0.132	--
O _s /O ₂ ^{20, 17}	75	0	0.126	--	0.134
O _s /O ₂ ^{20, 19}	100	0.184	0.184	0.184	0.184

¹⁶ Results of the (1 × 2) surface are represented, where water adsorbs in a linear fashion inflicting a 1-4 configuration on the occupied Al adsorption sites.

¹⁷ The 75 % coverage with water adsorption in 1-4 configuration with respect to two Al adsorption sites is presented.

¹⁸ The 75 % coverage with no water adsorption in 1-4 configuration is presented.

¹⁹ Results of the (1 × 1) surface are represented.

²⁰ The relaxation of the protonated O being a nearest neighbour of the indicated Al adsorption site is given.

The subscript number indicates that layer number starting from the surface. The bold numbers represent lateral movement induced by OH at an adsorption site. Interlayer distances were computed by averaging over all atoms within one layer. The only exception to this is the O_s of O_s-H.

Table SM3:

Comparison of inter layer distances in Å of different water coverage is presented for adsorption sites not in 1-4 configuration.

Inter layer spacing [Å]	Coverage [%]	Al _{1s}	Al _{2s}	Al _{3s}	Al _{4s}
Al ₁ /O ₂	25	0.112	0.742	0.125	--
Al ₁ /O ₂	50	0.755	--	0.755	--
Al ₁ /O ₂ ²¹	50	--	0.079	--	0.079
Al ₁ /O ₂ ²²	75	--	--	0.747	--
Al ₁ /O ₂ ²³	75	--	0.778	0.782	0.782
O _s /O ₂ ²⁴	25	0	0.100	0	0
O _s /O ₂ ²⁴	50	0.094	--	0.095	--
O _s /O ₂ ^{24, 22}	75	--	--	0.112	--
O _s /O ₂ ^{24, 23}	75	--	0.150	0.153	0.151

²¹ Results of a (1 x 2) cell are represented, where water adsorbs in a linear fashion inflicting a 1-4 configuration on the occupied Al adsorption sites.

²² The 75 % coverage with water adsorption in 1-4 configuration with respect to two Al adsorption sites is presented.

²³ The 75 % coverage with no water adsorption in 1-4 configuration is presented.

²⁴ The relaxation of the protonated O being a nearest neighbour of the indicated Al adsorption site is given.

The subscript number indicates that layer number starting from the surface. The bold numbers represent lateral movement induced by OH at an adsorption site. Interlayer distances were computed by averaging over all atoms within one layer. In case of the O_s-H adsorption site the averaging was done with respect to the none protonated O_s counterparts.

Table SM4:

The influence of the 1-4 configuration with respect to structural and vibrational properties of CO and the adsorbed water molecules at total surface coverage of 50 % and 75 % are presented.

	(2 x 2)	(2 x 2)	(2 x 2)	(2 x 2)
H ₂ O coverage [%]	25	25	50	50
CO coverage [%]	25	25	25	25
Species in 1-4 configuration	free adsorption site	CO	OH	CO
	A	B	C	D
r_{C-O} [Å]	1.148	1.148	1.148	1.147
r_{Al-C} [Å]	2.161	2.175	2.164	2.170
r_{Al-OH} [Å]	1.731	1.735	1.730 ²⁵	1.730
r_{O-H} [Å]	0.971	0.972	0.971 ²⁵	0.971
r_{Os-H} [Å]	0.985	0.982	0.984 ²⁵	0.984
ν_{C-O} [cm ⁻¹]	2225	2232	2233	2240
Δ_{C-O} [cm ⁻¹]	55	62	63	70
ν_{O-H} [cm ⁻¹]	3936	3925	3935	3914
ν_{Os-H} [cm ⁻¹]	3696	3740	3698	3733
CO adsorbtion energy [eV]	0.57	0.44	0.51	0.52

²⁵ Average values are presented.

Table SM5:

The influence of the 1-4 configuration with respect to structural and vibrational properties of CO and the adsorbed water molecules at total surface coverage of 100 %.

	(1 x 2)	(1 x 2)	(2 x 2)
H ₂ O coverage [%]	50	50	75
CO coverage [%]	50	50	25
Species in 1-4 configuration	OH	CO	CO/ OH
	E	F	G
r_{C-O} [Å]	1.149	1.150	1.147
r_{Al-C} [Å]	2.167	2.195	2.177
r_{Al-OH} [Å]	1.738	1.737	1.728 ^{26,27} 1.732 ²⁸
r_{O-H} [Å]	0.971	0.972	0.972 ^{26,27} 0.973 ²⁸
r_{Os-H} [Å]	0.984	0.982	0.984 ^{26,27} 0.982 ²⁸
ν_{C-O} [cm ⁻¹]	2227	2225	2242
Δ_{C-O} [cm ⁻¹]	57	52	72
ν_{O-H} [cm ⁻¹]	3922	3915	3921 ^{26,27} 3914 ²⁸
ν_{Os-H} [cm ⁻¹]	3683	3720	3701 ^{26,27} 3747 ²⁸
CO adsorption energy [eV]	0.51	0.44	0.48

²⁶ Average values are presented.

²⁷ Al-OH adsorption site in 1-4 position is presented.

²⁸ Al-OH adsorption site inflicting 1-4 position upon CO adsorption is presented.

Table SM6:

Comparison of inter layer distance in Å with respect to the CO adsorption site in 1-4 configuration (Al CO 1-4) and the CO site which is not in 1-4 configuration (Al CO) are given. In addition the OH adsorption site (Al OH Inflicting 1-4) inflicting a 1-4 arrangement onto adsorption sites of OH (Al OH 1-4), CO or the free Al adsorption site (Al Free 1-4) as well as the free adsorption site not in 1-4 configuration are shown.

Inter layer spacing [Å]	Coverage H ₂ O/CO[%]	Al CO 1-4	Al CO	Al OH 1-4	Al OH Inflicting 1-4	Al Free 1-4	Al Free
Al ₁ /O ₂	A 25/25	--	0.364	--	0.748	-0.342	0.093
Al ₁ /O ₂	B 25/25	0.301	--	--	0.728	--	0.046 ³²
Al ₁ /O ₂	C 50/25		0.344	0.694	0.693	--	0.030
Al ₁ /O ₂	D 50/25	0.312	--	0.732 ^{30,31}	0.732 ³⁰	-0.337	--
Al ₁ /O ₂	E 50/50 ²⁹	--	0.279	0.651	0.651	--	--
Al ₁ /O ₂	F 50/50 ²⁹	0.233	--	--	0.655	--	--
Al ₁ /O ₂	G 75/25	0.295	--	0.681 ³²	0.712	--	--

²⁹ Results of a 1x2 super cell are represented.

³⁰ This Al adsorption site is inflicting 1-4 configuration upon CO.

³¹ This Al adsorption site is inflicting 1-4 configuration upon the free Al adsorption site.

³² An average value of the two equivalent adsorption site is presented.

The subscript number indicates the layer number starting from the surface. Interlayer distances were computed by averaging over all atoms within one layer.

Table SM7:

Comparison of inter layer distance in Å of the O_S adsorption site in 1-2 position with respect to the OH adsorption site inflicting a 1-4 arrangement (Al O_S-H inflicting 1-4) to CO another OH or the free Al adsorption are shown. In addition the O_S site in 1-2 arrangement to its OH adsorption site which is in 1-4 configuration (Al O_S-H 1-4), caused by a linear adsorption of water is presented. Interlayer distances were computed by averaging over all atoms within one layer. In case of the O_S-H adsorption site the averaging was done with respect to the none protonated O_S counterparts.

Inter layer spacing [Å]	Coverage H ₂ O/CO[%]	Al O _S -H inflicting 1-4	Al O _S -H 1-4
O _S /O ₂	A 25/25	--	0.089
O _S /O ₂	B 25/25	0.094	--
O _S /O ₂	C 50/25	0.104	0.116 ³⁴
O _S /O ₂	D 50/25	0.091	0.107
O _S /O ₂	E 50/50 ³³	--	0.120
O _S /O ₂	F 50/50 ³³	0.101	--
O _S /O ₂	G 75/25	0.118 ³⁵	0.089

³³ Results of a (1 × 2) surface are represented.

³⁴ Nearest neighbour to the free adsorption site.

³⁵ An average value of the two equivalent adsorption site is presented.

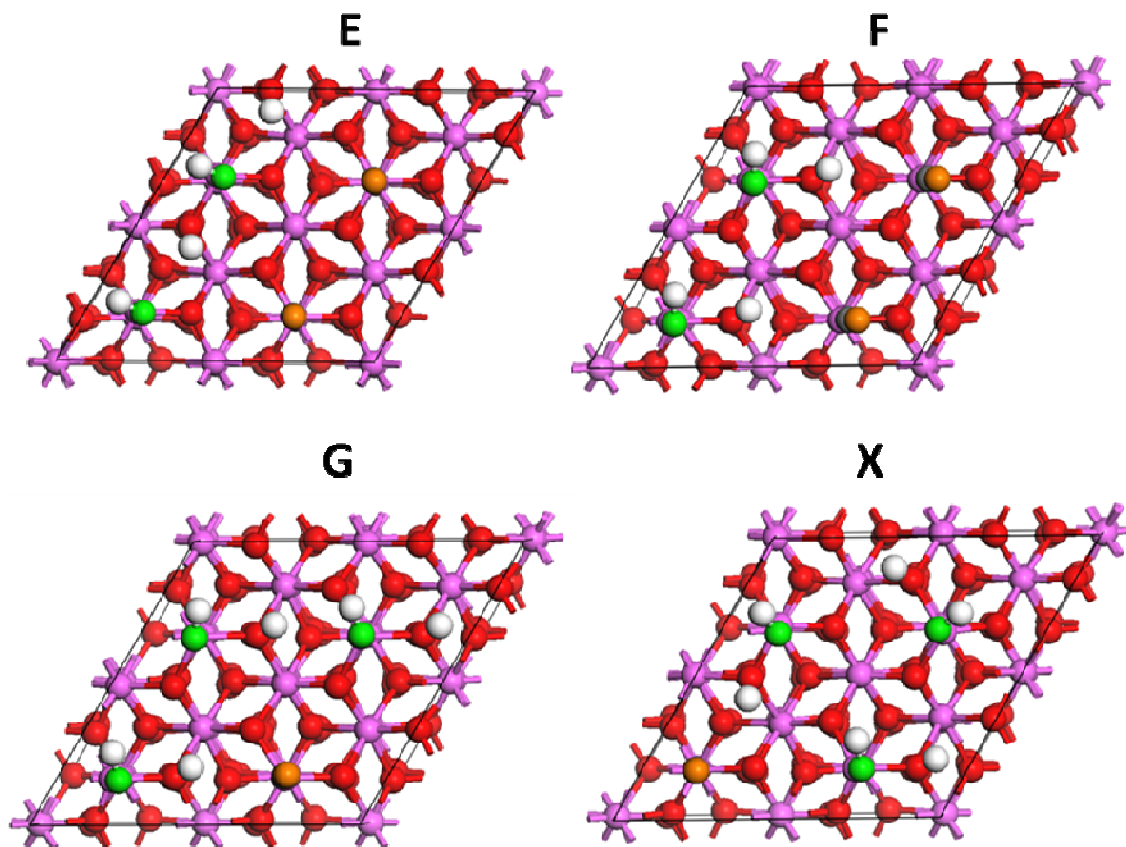


Figure SM 1:

- E 50 % hydroxylation 50 % CO coverage, 1-4 inflicted on the OH adsorption site
- F 50 % hydroxylation 50 % CO coverage, 1-4 inflicted on the CO adsorption site
- G 75 % hydroxylation 25 % CO coverage, 1-4 inflicted on the CO and the OH adsorption sites
- X 75 % hydroxylation 25 % CO coverage, 1-4 inflicted three times on the CO adsorption site

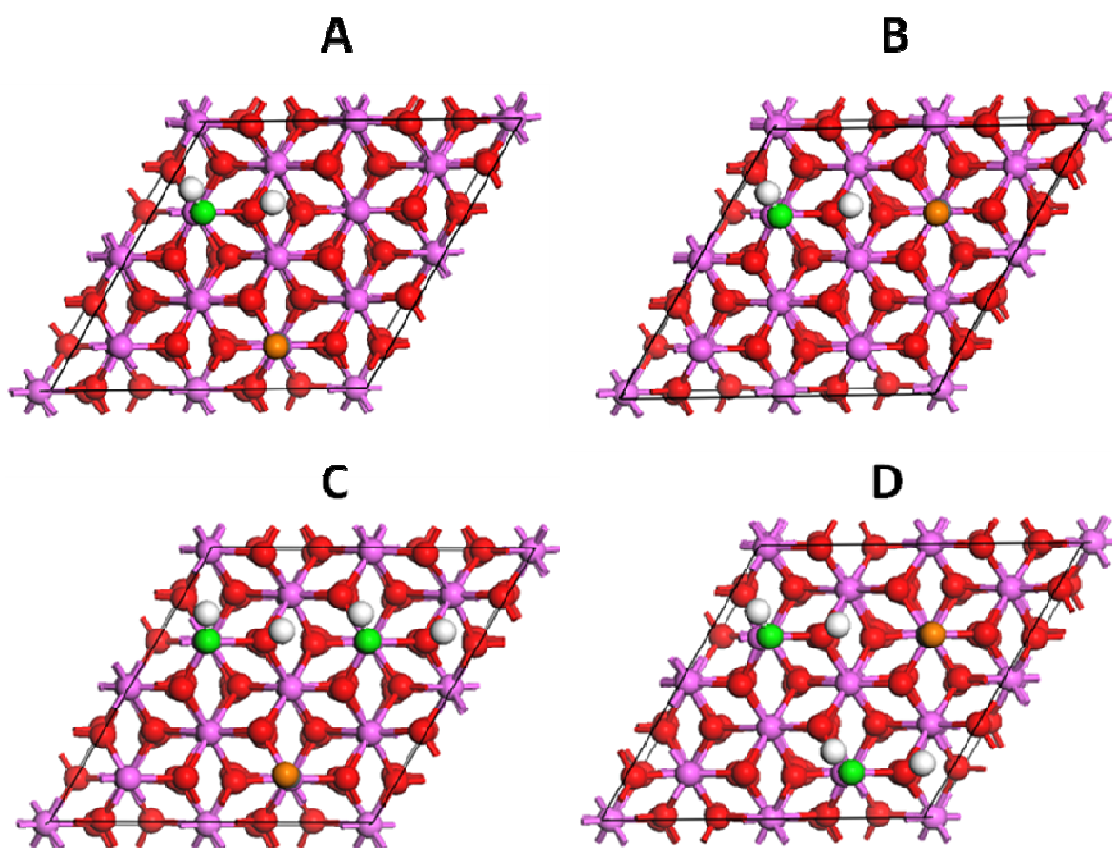


Figure 12:

- (a) 25 % hydroxylation, 1-4 adsorbed on the free Al adsorption site.
- (b) 25 % hydroxylation, 1-4 adsorbed on the CO adsorption site.
- (c) 50 % hydroxylation, 1-4 adsorbed on two OH adsorption sites.
- (d) 50 % hydroxylation, 1-4 adsorbed on the CO and the free adsorption site. All results are on the 25% CO coverage.